Ab initio prediction of the vibration-rotation-tunneling spectrum of HCl–(H$_2$O)$_2$

P. E. S. Wormer, G. C. Groenenboom, and A. van der Avoird
Institute of Theoretical Chemistry, NSR/RIM, University of Nijmegen, Toernooiveld, 6525 ED Nijmegen, The Netherlands

Quantum calculations of the vibration-rotation-tunneling (VRT) levels of the trimer HCl–(H$_2$O)$_2$ are presented. Two internal degrees of freedom are considered—the rotation angles of the two nonhydrogen-bonded (flipping) hydrogens in the complex—together with the overall rotation of the trimer in space. The kinetic energy expression of van der Avoird *et al.* [J. Chem. Phys. **105**, 8034 (1996)] is used in a slightly modified form. The experimental microwave geometry of Kisiel *et al.* [J. Chem. Phys. **112**, 5767 (2000)] served as input in the generation of a planar reference structure. The two-dimensional potential energy surface is generated *ab initio* by the iterative coupled-cluster method based on singly and doubly excited states with triply excited states included noniteratively [CCSD(T)]. Frequencies of vibrations and tunnel splittings are predicted for two isotopomers. The effect of the nonadditive three-body forces is considered and found to be important. © *2001 American Institute of Physics.* [DOI: 10.1063/1.1388203]

I. INTRODUCTION

Detailed information on the pair and three-body interactions in water can be obtained from the high-resolution spectra of the water dimer, trimer, and larger clusters.[1–16] Dynamical calculations[17,18] are needed to extract this information from these spectra. Especially the far-infrared and microwave spectra of such clusters, which measure the frequencies of the intermolecular vibrations and tunneling splittings, turn out to be extremely sensitive to the shape of the intermolecular potential surface.[19–22]

Another interesting problem is the solvation of HCl in water. Also this process, and the HCl–water interactions by which it is determined, can be investigated by studying the internal dynamics and the corresponding spectra of small HCl–water clusters. It is known that HCl is a strong acid that dissociates easily into H$^+$ and Cl$^-$ when dissolved in excess water. As such the HCl–water clusters are of interest in the study of acidity and the kinetics of proton transfer. The HCl–water clusters have been studied extensively, too, because of the role they play in the ozone depletion cycle. The Cl radical catalytically converts ozone to oxygen.[23] This radical may be formed from HCl adsorbed on the surface of hexagonal water ice clusters that appear in polar stratospheric clouds.[24,25] Because of this role the HCl–water clusters have drawn much attention of molecular dynamicists[26–29] and experimentalists.[30–34]

In this work we study the trimer HCl–(H$_2$O)$_2$ and one of its isotopomers. This trimer is similar to the water trimer in that it is also strongly hydrogen-bonded. The interactions and internal motions in the water trimer received much attention.[21,35–65] It is the general conclusion of these papers that only the nonhydrogen-bonded hydrogens in the water trimer show large amplitude motions and tunnel through the plane of the semirigid hydrogen-bonded network. The vibrations of the network are much stiffer than of the three nonhydrogen-bonded (external) hydrogens. It is likely that HCl–(H$_2$O)$_2$ will show similar behavior. That is, the hydrogen bonds will form a rather rigid and almost planar network and the two external hydrogens will show large amplitude motions and tunnel through this plane. From the microwave observations of rotational spectra[67] it is deduced that the hydrogen-bonded part of the present complex is indeed nearly planar. Since to date no experimental (far-)infrared results are available for this complex, the assumption that the two external hydrogen atoms tunnel appreciably through the plane, is not yet proven experimentally. However, one of the main purposes of the present work is to investigate whether this is the case. Further we will compute the vibration-rotation-tunneling (VRT) spectrum as a guide to future spectroscopic studies.

Even more than in the water trimer, the three-body effects are considerable[66] in the very polar system HCl–(H$_2$O)$_2$. Consequently, the results of a study on the trimer will be useful for larger clusters, as the most important interactions, the pair- and the three-body interactions, are present in the trimer.

In this study of the internal motions in HCl–(H$_2$O)$_2$ we apply a dynamical model that is very similar to the one that was developed earlier for the water trimer[53,54,61] in order to interpret and understand the high-resolution far-infrared spectra.[11,12] An important difference with the water trimer is that the present complex does not have three equal monomers on the vertices of an equilateral triangle. So, in this paper we will have to modify the earlier model somewhat. Again we consider $J \neq 0$ states and Coriolis coupling between the internal motions and the overall rotation of the trimer. The VRT energy levels will be presented. As far as we are aware, the vibration-tunneling levels have not yet been measured or calculated earlier. Kisiel *et al.*[67] measured recently the rotational spectrum of HCl–(H$_2$O)$_2$ and several
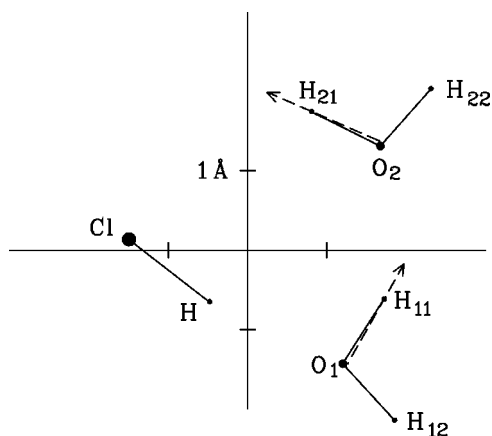
FIG. 1. Planar reference geometry. The rotation axes are dashed and the direction of positive rotation is given. The two water molecules are characterized by $r_{OH}=0.9650$ Å and $\angle HOH=104.784°$, while $r_{HCl}=1.2839$ Å. A distance of 1 Å is marked on the axes to give an indication of the bond lengths. The numerical values of the coordinates are listed in Table I.

of its isotopomers and extracted the Cartesian coordinates of the atoms from the rotational constants. A small modification of these coordinates yields a planar reference geometry, which is essential to our model.

We end the introduction with an outline of the work. It consisted of the following consecutive steps: First, a planar reference geometry of the trimer was obtained from the not completely planar experimental coordinates. Then an atomic orbital basis set was chosen and used to generate by the CCSD(T) (coupled cluster single and double with noniterative triples) method a two-dimensional potential energy surface (PES). This surface was fitted and applied in the solution of the nuclear motion problem. The form of the kinetic energy operator appearing in this problem is similar, but not identical, to the operator used in the water trimer, which is why we sketch briefly its form. Finally the Hamilton matrix was diagonalized and the rovibrational states were obtained. They are discussed in the one but last section of this paper. The last section contains the conclusions.

II. THEORY

In Fig. 1 we show a planar reference geometry of the trimer, which is close to the geometry proposed by Kisiel et al.[67] on the basis of their measured rotational spectra. Below we will discuss how we obtained this reference geometry from the experimental geometry. We see a hydrogen-bonded water dimer inside the complex with the first water molecule acting as hydrogen donor to the second. Further the HCl monomer donates a hydrogen to the first water molecule, while the second water molecule donates a hydrogen to the HCl molecule. The latter hydrogen bond is strongly bent and much weaker than the other two bonds.[67] In analogy to the case of the water trimer[53,54] we expect that the two nonbonded hydrogens (H₁,₂ and H₂,₂) can tunnel through the plane of the trimer. In this section we describe a model for this tunneling motion in which the hydrogen-bonded network is kept rigid and the free hydrogens H₁,₂ and H₂,₂ rotate, see Fig. 1. A free hydrogen rotates around the axis pointing from the center of mass of its water molecule to its hydrogen-

bonded hydrogen atom. Before discussing the choice of the planar reference geometry we first review the form of the kinetic energy operator for this motion, because it dictates to some extent the choice of the reference geometry.

A. Kinetic energy operator

We follow closely the derivation given in Ref. 53 for the water trimer. The hydrogen-bonded trimers $(H_2O)_3$ and $(D_2O)_3$ are oblate symmetric tops due to the averaging over six symmetry equivalent minima in a three-dimensional potential energy surface. The three degrees of freedom of this surface are rotation angles of the nonhydrogen-bonded hydrogen atoms. During their rotation the three hydrogen nuclei flip through the plane of the hydrogen-bonded skeleton and the system tunnels from one equivalent minimum to another. In previous articles from our group[53,54] a Hamiltonian was derived describing this three-dimensional tunneling motion. The overall rotation of the trimer was also included in the model, so that states with total angular moment quantum number $J\neq 0$ could be studied. At first the model was applied to the symmetric, isotopically pure, trimers and later to some less symmetric isotopomers.[61] The model gives a consistent assignment of all bands measured to date.

Since in the water trimer *three* protons are tunneling and since this trimer is a symmetric top, while the present trimer is an asymmetric top, we must adapt the derivation somewhat. The derivation of Ref. 53 starts by introducing internal and external (Euler) angles as generalized coordinates. Then the metric tensor of these coordinates is derived and the analytic inverse of this tensor is substituted into the Podolsky form[68] of the kinetic energy. The three external Euler angles are designated α, β, and γ. The first two are the spherical polar angles of the z-axis (perpendicular to the plane of the trimer) with respect to the lab frame. The third angle, γ gives a rotation of the trimer around the z-axis. The internal angles χ_1 and χ_2 are the rotation angles of the free hydrogens around the axes described above—the dashed lines in Fig. 1.

In order to present the kinetic energy operator, we must introduce some auxiliary quantities. The vector $\mathbf{v}_\nu$ is the position vector of the center of mass of monomer ν in the frame shown in Fig. 1. The mass of monomer ν is m_ν. We approximate the exact operator in the same way as in Ref. 53 [Eq. (A37)] and assume that the part $\mathbf{I}_\nu^{eff}$ of the inertia tensor of the trimer may be neglected. This neglect does not affect at all the dominant term in the Hamiltonian [(the first term of H^{int} in Eq. (5) below] and has a small effect on the other kinetic energy terms. Accordingly we write this tensor as

$$(I_M)_{kl}\equiv\sum_{\nu=1}^{3}m_\nu(\delta_{kl}v_\nu^2-v_{\nu,k}v_{\nu,l}),\qquad(1)$$

where v_ν is the length of $\mathbf{v}_\nu$. Note that $\mathbf{I}_M$ is the inertia tensor of a system of three ''pseudo'' particles that have monomer masses and are positioned at the mass centers of the monomers. We will choose our reference geometry such that the tensor $\mathbf{I}_M$ is diagonal.

The kinetic energy operator contains $\mathbf{J}=(J_x,J_y,J_z)$, which is the total angular momentum operator. It has the usual form of a body-fixed rigid rotor angular momentum operator satisfying anomalous commutation relations.

TABLE I. Planar reference geometry (Å). The axes are principal axes of the tensor $\mathbf{I}_M$ [Eq. (1)] with rotational constants: $1/(2I_M)_{xx} = A = 7112.62$ MHz, $1/(2I_M)_{yy} = B = 3250.18$ MHz, $1/(2I_M)_{zz} = C = 2230.80$ MHz. The coordinates are depicted in Fig. 1.

	x	y	z
O_1	1.151 15	−1.466 67	0.0
$H_{1,1}$	1.696 41	−0.670 48	0.0
$H_{1,2}$	1.781 85	−2.197 04	0.0
O_2	1.707 32	1.259 21	0.0
$H_{2,1}$	0.859 92	1.720 86	0.0
$H_{2,2}$	2.369 92	1.960 76	0.0
Cl	−1.490 27	0.182 72	0.0
H	−0.499 98	−0.634 41	0.0

TABLE II. Coordinates obtained by rotating the two water molecules in the reference geometry of Table I over $\chi_1 = 30.8°$ and $\chi_2 = -40.0°$, respectively. The experimental coordinates of Ref. 67 are given in the last three columns. Units: Å.

	Rotated			Experiment		
O_1	1.1577	−1.4706	−0.0279	1.0921	−1.5357	−0.0429
$H_{1,1}$	1.6964	−0.6705	0.0000	1.6425	−0.7434	−0.0178
$H_{1,2}$	1.6777	−2.1340	0.4420	1.5711	−2.1851	0.4863
O_2	1.7128	1.2707	0.0350	1.7739	1.1944	0.0404
$H_{2,1}$	0.8599	1.7209	0.0	0.9136	1.6313	0.0511
$H_{2,2}$	2.2835	1.7784	−0.5547	2.3373	1.7728	−0.4881
Cl	−1.4903	0.1827	0.0	−1.4815	0.1630	0.0009
H	−0.5000	−0.6344	0.0	−0.5446	−0.7145	−0.0228

Further we designate the unit vectors along the water rotation axes—the dashed lines in Fig. 1—by $\mathbf{h}_\nu = (\cos \xi_\nu, \sin \xi_\nu, 0)^T$. From Table I it is easy to get $\xi_1 = 58.827°$ and $\xi_2 = 154.650°$. The water inertia tensor on basis of principal monomer axes is $\mathrm{diag}(I_b, I_a, I_c)$. We rotate the principal axis frames of both monomers around their respective c-axes (perpendicular to the plane of the molecule) over an angle ϕ, which is the angle between the b-axis (the bisector of the molecule) and the vector $\mathbf{h}_\nu$. From the coordinates in Table I we obtain $\phi = 55.623°$. In the rotated frame the water monomer inertia tensor becomes

$$
\begin{pmatrix} I_{xx} & I_{xy} & 0 \\ I_{xy} & I_{yy} & 0 \\ 0 & 0 & I_{zz} \end{pmatrix} \equiv \mathbb{R}_z(-\phi) \begin{pmatrix} I_b & 0 & 0 \\ 0 & I_a & 0 \\ 0 & 0 & I_c \end{pmatrix} \mathbb{R}_z(\phi),
$$
(2)

where $\mathbb{R}_z(\phi)$ is a rotation matrix representing an active rotation around the z-axis over ϕ. We will see that the energy eigenvalues are dominated by the magnitude of the tensor element I_{xx}; it is the moment of inertia corresponding to rotation around $\mathbf{h}_\nu$. Its numerical value is given by $1/(2I_{xx}) = 21.1135$ cm^{-1} (for the protonated trimer).

We introduce the angular momentum operator $\mathbf{j}_\nu$, which generates the rotation around $\mathbf{h}_\nu$,

$$
\mathbf{j}_\nu \equiv -\frac{i}{I_{xx}} \begin{pmatrix} I_{xx} \cos \xi_\nu - I_{xy} \sin \xi_\nu \cos \chi_\nu \\ I_{xx} \sin \xi_\nu + I_{xy} \cos \xi_\nu \cos \chi_\nu \\ I_{xy} \sin \chi_\nu \end{pmatrix} \frac{\partial}{\partial \chi_\nu},
$$

$$\nu = 1,2.$$
(3)

These operators are non-Hermitian due to the presence of $\cos \chi_\nu$ and $\sin \chi_\nu$ in their definition. We write $\mathbf{j} \equiv \mathbf{j}_1 + \mathbf{j}_2$. As the last auxiliary quantity we introduce the Hermitian operator $\mathbf{j}^H \equiv \mathbf{j} + \mathbf{j}^\dagger$.

In terms of these auxiliary quantities the Hamiltonian becomes finally[53]

$$H = H^{\mathrm{rot}} + H^{\mathrm{Cor}} + H^{\mathrm{int}}$$
(4)

with

$$H^{\mathrm{rot}} = AJ_x^2 + BJ_y^2 + CJ_z^2,$$

$$H^{\mathrm{Cor}} = -A J_x j_x^H - B J_y j_y^H - C J_z j_z^H,$$
(5)

$$
H^{\mathrm{int}} = -\frac{1}{2} \sum_{\nu=1}^{2} \frac{1}{I_{\nu,xx}} \frac{\partial^2}{\partial \chi_\nu^2} + A j_x^\dagger j_x + B j_y^\dagger j_y + C j_z^\dagger j_z
$$

$$+ V(\chi_1, \chi_2).$$

The sum over ν runs over the two water molecules and we attached the index ν to $I_{\nu,xx}$ to allow for different isotopes. Observe that this tensor element occupies the position of the mass in the usual kinetic energy operators, which explains its importance. The potential $V(\chi_1, \chi_2)$ will be introduced below.

B. Reference geometry

The geometry of the hydrogen-bonded system HCl–(H$_2$O)$_2$ was determined by Kisiel and co-workers.[67] They measured microwave spectra of different isotopomers in different rotational states and extracted atomic coordinates from their spectra. The complex was found to be almost, but not completely, planar, the main exception being the two water protons that do not participate in a hydrogen bond. One proton was found above the plane of the complex and the other below it. The other atoms are close to the xy plane, but not in it, see Table II. In our model we assume a rigid planar hydrogen-bonded network Cl–H–M$_1$–H$_{1,1}$– M$_2$–H$_{2,1}$, where M$_1$ and M$_2$ are the centers of mass of the water monomers 1 and 2. The free hydrogens are rotated out of this plane by rotations over χ_1 and χ_2, but also the oxygens move slightly out of the plane by these rotations. We extracted from the experimental data a planar structure of the hydrogen-bonded framework and the angles χ_1 and χ_2 of the external hydrogens that give optimum rotational constants. In doing this we first computed the rotational constants from the experimental coordinates, $A_{\mathrm{exp}} = 6853.6$, $B_{\mathrm{exp}} = 3187.5$, and $C_{\mathrm{exp}} = 2185.8$ MHz, where we used the masses H: 1.007 825 2 u, ^{16}O: 15.994 915 0 u, and ^{35}Cl: 34.968 851 0 u. We put the index "exp" to these constants because they are calculated from the experimental coordinates; we do not imply that these constants were directly observed. To obtain the planar reference structure we minimized the root mean square error (RMS): $R \equiv \frac{1}{3} [\Delta A^2 + \Delta B^2 + \Delta C^2]^{1/2}$, where ΔA stands for the difference between the experimental and our A rotational constant and likewise for B and C. The optimum rotational constants, which occur for the angles $\chi_1 = 30.8°$

and $\chi_2 = -40.0°$, are $A = 6853.6$, $B = 3187.4$, and $C = 2185.7$ MHz with $R = 0.05$ MHz. The corresponding Cartesian coordinates are given in Table I.

At this point we note already that the surface has an *ab initio* minimum for $\chi_1 = 57°$ and $\chi_2 = -26°$. The rotational constants for these angles are $A = 6841.4$, $B = 3185.5$, and $C = 2187.3$ MHz which have a RMS of 4.1 MHz = 1.4×10^{-4} cm^{-1}.

After having found the reference geometry, we performed an overall rotation of the system in the xy-plane by means of the eigenvectors of $\mathbf{I}_M$ [Eq. (1)]. This rotation gives reference coordinates that diagonalize $\mathbf{I}_M$. The corresponding rotational constants A, B, and C (given in the caption of Table I) deviate 3.6%, 1.9%, and 2.0% from the values A_{exp}, B_{exp}, and C_{exp}, respectively. These percentages give an indication of the error introduced by neglecting $\mathbf{I}_\nu^{eff}$ in the total inertia tensor.

III. CALCULATION AND FIT OF THE POTENTIAL ENERGY SURFACE

A. Calculation

All our *ab initio* calculations were done by the CCSD(T) method. They were performed with the aid of the program MOLPRO.[69] By default MOLPRO excites from the highest four occupied (valence) molecular orbitals for the HCl monomer as well as for the H₂O monomer. We used this default. In the case of the trimer this means that excitations are from the highest twelve occupied orbitals, while for the dimers excitation is from highest eight. We computed the following CCSD(T) interactions:

$$E(1,3) = E_A + E_B + E_C,$$
$$E(2,3) = E_{AB} + E_{BC} + E_{CA} - 2E(1,3), \qquad (6)$$
$$E(3,3) = E_{ABC} - E(1,3) - E(2,3),$$

where $E(N,3)$ denotes the N-body term in the trimer. All seven CCSD(T) energies $E_A, \ldots, E_{ABC}$ are computed in the trimer basis, thus correction for basis set superposition errors is automatically assured. Here A, B, and C label the monomers. Unless stated differently we will describe the potential energy surface (PES) by the sum of the pair interactions $E(2,3)$ plus the nonadditive term $E(3,3)$. Below we will show that the surface is symmetric under $(\chi_1, \chi_2) \rightarrow (-\chi_1, -\chi_2)$, which is due to the inversion symmetry E^*.

It is important for a reliable prediction of the tunneling splittings that barrier heights and widths in the PES are computed correctly. A good atomic orbital basis is crucial for this. In finding the basis we proceeded in two rounds. In the first round we scanned the surface with the moderately sized aug-cc-pVDZ basis.[70] In this basis we found the equilibrium to be close to $(\chi_1, \chi_2) = (60°, -30°)$ and we expect a tunneling from this minimum to $(\chi_1, \chi_2) = (-60°, 30°)$ through a barrier which has its maximum at $(\chi_1, \chi_2) = (0°, 0°)$. The barrier height in this small basis is 348.9 cm^{-1}. The same basis gives the lower barrier of 331.3 cm^{-1} in the second-order Møller–Plesset (MP2) approximation, which is why we did not use MP2 in our calculations.

TABLE III. CCSD(T) barriers (cm^{-1}) as a function of basis. The barrier is defined as $V(\chi_1 = 60°, \chi_2 = -30°) - V(\chi_1 = 0°, \chi_2 = 0°)$, where V is the two- plus three-body interaction.

Basis	Dimension	Barrier
aug-cc-pVDZ [a]	118	348.9
aug-cc-pVTZ [a]	257	311.0
cc-pVTZ [a]	164	285.0
6311++G(2d,2p) [a]	139	327.1
aug-cc-VDZ + bond [b]	184	328.6
EZPPBF(water)/aug-cc-pVTZ(Cl) [c]	174	313.3
EZPPBF(water)/6311++G(2d,2p)(Cl) [d]	156	308.1

[a]From Ref. 70.
[b]From Ref. 70, plus bond orbitals in hydrogen bond, s, p: $\alpha = 0.9, 0.3, 0.1$, d: $\alpha = 0.6, 0.2$.
[c]Water from Ref. 71 plus extra d ($\alpha = 0.6$) on oxygen; chlorine from Ref. 70.
[d]Water from Ref. 71; chlorine from Ref. 70, plus extra f ($\alpha = 0.7$) on chlorine.

In the second round we started by first computing the barrier height in the rather large aug-cc-pVTZ basis[70] and searched for smaller, more economical, bases that could reproduce this height. The different heights obtained in different basis sets are shown in Table III. Assuming that the value of 311.0 cm^{-1} obtained in the largest (i.e., the aug-cc-pVTZ) basis is the best approximation to the true value, we find that the 156-dimensional basis: EZPPBF on water and $6311++G(2d,2p)+f$ on Cl gives a good price/performance ratio. The water part of this basis is due to the van Duijnevelts.[71] The letters EZ refer to the extended zeta set $(10s, 6p/5s, 3p)$ on O and $(4s/2s)$ on H. The letters PP refer to two polarization functions on H and O. The letter B refers to an s and p orbital ($\alpha_s = \alpha_p = 0.6$) in the three hydrogen bonds, i.e., halfway the Cl–H$_{2,1}$, H–O$_1$, and H$_{1,1}$–O$_2$ bonds. The letter F refers to a single f orbital on O. We used the same basis for the HCl hydrogen as for the water hydrogens. The chlorine part of the basis is the $6311++G(2d, sp)$ basis from Ref. 72 augmented with an f orbital with exponent $\alpha = 0.7$. We used this basis to compute the PES on 50 points in the range from $-110°$ to $110°$. These *ab initio points* are made available via EPAPS.[73]

B. Fit

We fitted the total interaction $E(2,3) + E(3,3)$ as well as only the two-body interaction $E(2,3)$, cf. Eq. (6). Writing V for either potential we note that because of symmetry $V(\chi_1, \chi_2) = V(-\chi_1, -\chi_2)$. We used for the fit the reproducing kernel Hilbert space interpolation method of Ho and Rabitz,[74] which we slightly modified to build in the symmetry. In order to use the reproducing kernel (r.k.) proposed by these workers for anglelike variables we define the scaled and shifted coordinates $x(\chi_1) = \frac{1}{2}(\chi_1/\chi_{max} + 1)$ and $y(\chi_2) = \frac{1}{2}(\chi_2/\chi_{max} + 1)$, with $\chi_{max} = 110°$ such that $0 \leq x, y \leq 1$. The potential is expanded as

$$V(\chi_1, \chi_2) = \sum_{i=1}^{50} c_i [q_2^n(x, x_i) q_2^n(y, y_i)$$
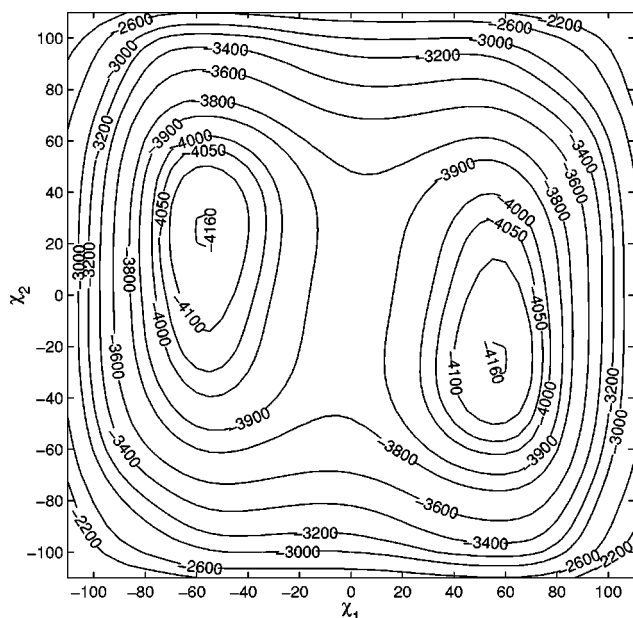$$+ q_2^n(1-x, x_i) q_2^n(1-y, y_i)], \qquad (7)$$

FIG. 2. Contour diagram of the interaction energy (cm^{-1}) $V(\chi_1,\chi_2)$.

where the r.k. $q_2^n(x,x')$ is the polynomial of degree $2n-1$ for $x<x'$ and of degree $n-1$ for $x>x'$ as defined in Eq. (23) of Ref. 74. We find that $n=3$ gives a sufficiently smooth fit. The coordinates x_i and y_i are related to the coordinates of the 50 *ab initio* points by $x_i \equiv x(\chi_{1i})$ and $y_i = y(\chi_{2i})$. The 50 expansion coefficients c_i are obtained as the solutions of the linear equations that arise from the conditions $V_i = V(\chi_{1i},\chi_{2i})$, where the values V_i are the CCSD(T) interaction energies. Since the condition number of the set of linear equations is about 5×10^{13}, we do not need to use a regularization method as discussed in section 2C of Ref. 74.

The second term in Eq. (7) enforces the symmetry since $x(-\chi_1)=1-x(\chi_1)$ and $y(-\chi_2)=1-y(\chi_2)$. Initially we tried to obtain a fit of the correct symmetry by simply adding the symmetry related points to the *ab initio* data, while fitting without the second term in Eq. (7). However, this yields a fit which is only approximately symmetric.

See Fig. 2 for a contour diagram of the fitted potential. The value D_e of the depth of the well at $\chi_1=57°$ and $\chi_2=-26°$ is 4164.26 cm^{-1}. The value for the saddle point $\chi_1=\chi_2=0°$ is -3851.73 cm^{-1}, thus the barrier height is 312.53 cm^{-1}. The minimum in the two-body potential is at $\chi_1=54°$ and $\chi_2=-26°$. Its depth D_e is 3629.17 cm^{-1} and its value at $\chi_1=\chi_2=0°$ is -3378.41 cm^{-1}, which makes for a two-body barrier height of 250.76 cm^{-1}. This height is about 62 cm^{-1} lower than the height in the total two- plus three-body PES.

IV. THE NUCLEAR MOTION PROBLEM

We start this section by discussing the computation of the matrix of the Hamiltonian in a product basis of sinc and rigid rotor functions. Under the condition that the total inertia tensor does not depend on χ_1 and χ_2, the volume element associated with χ_1 and χ_2 is constant and only the usual weight $\sin\beta$ must be included in the integrations, where β is

the second of the three Euler angles describing the overall rotation. In the solution of the nuclear motion problem we use a basis of Wigner D-matrix elements[75] $D_{MK}^{(J)}(\alpha,\beta,\gamma)^*$ times a product $\xi_n(\chi_1)\xi_m(\chi_2)$ of discrete variable representation (DVR) sinc functions. A DVR sinc function has the form,[76,77]

$$\xi_n(\chi) = \Delta^{-1/2}\frac{\sin\pi(\chi/\Delta-n)}{\pi(\chi/\Delta-n)}. \tag{8}$$

These functions have the DVR property, $\xi_n(m\Delta) = \Delta^{-1/2}\delta_{n,m}$ and are located on an equidistant grid with spacing Δ, which we take to be the same for the two angles throughout this paper. The index n counts the points on the grid. The potential energy matrix elements are approximated by a quadrature on this grid. As a result the potential energy matrix is diagonal

$$\langle\xi_{n'}(\chi_1)\xi_{m'}(\chi_2)|V(\chi_1,\chi_2)|\xi_n(\chi_1)\xi_m(\chi_2)\rangle$$
$$= \delta_{n'n}\delta_{m'm}V(n\Delta,m\Delta). \tag{9}$$

All multiplicative (local) operators are evaluated in this approximation.

Since the sinc functions are orthonormal it follows that

$$\left\langle\xi_{n'}(\chi_1)\xi_{m'}(\chi_2)\left|\frac{\partial^2}{\partial\chi_1^2}\right|\xi_n(\chi_1)\xi_m(\chi_2)\right\rangle$$
$$= \delta_{m'm}\left\langle\xi_{n'}(\chi_1)\left|\frac{\partial^2}{\partial\chi_1^2}\right|\xi_n(\chi_1)\right\rangle, \tag{10}$$

and a similar expression for $\partial^2/\partial\chi_2^2$. The second derivatives are given analytically by[76,77]

$$\left\langle\xi_{n'}\left|\frac{\partial^2}{\partial\chi^2}\right|\xi_n\right\rangle = \begin{cases} -\dfrac{\pi^2}{3\Delta^2} & \text{for } n'=n \\[2mm] -\dfrac{2(-1)^{n'-n}}{(n'-n)^2\Delta^2} & \text{for } n'\neq n. \end{cases} \tag{11}$$

The matrix elements of the operators $j_{\nu i}^\dagger j_{\nu i}$, $(i=x,y,z)$ can be computed by substitution of a resolution of identity in the sinc basis between functions and differential operators. To show this we write briefly $j_{\nu x}=-i(a\partial/\partial\chi+b\cos\chi\partial/\partial\chi)$, where the constants a and b are given by Eq. (3). The operator $j_{\nu x}^\dagger j_{\nu x}$ can be rewritten in different ways. Since the resolution of the identity in the sinc basis is an approximation, the best results are obtained by an expression with the local functions $\sin\chi$ and $\cos\chi$ on the outside. This is because local functions are diagonal in the sinc basis, so that only one term of the resolution of identity survives. Further we require the expression to be manifestly Hermitian. Thus, we write

J. Chem. Phys., Vol. 115, No. 8, 22 August 2001

Spectrum of HCl–(H₂O)₂   3609

$$j_{\nu x}^{\dagger} j_{\nu x} = -a^2 \frac{\partial^2}{\partial \chi^2} - b^2 \left(\cos \chi \frac{\partial^2}{\partial \chi^2} \cos \chi - \sin^2 \chi \right.$$

$$- \sin \chi \frac{\partial}{\partial \chi} \cos \chi + \cos \chi \frac{\partial}{\partial \chi} \sin \chi \bigg)$$

$$- ab \left(\cos \chi \frac{\partial^2}{\partial \chi^2} + \frac{\partial^2}{\partial \chi^2} \cos \chi - \sin \chi \frac{\partial}{\partial \chi} + \frac{\partial}{\partial \chi} \sin \chi \right). \tag{12}$$

The expression for $j_{\nu y}^{\dagger} j_{\nu y}$ is completely analogous, and for $j_{\nu z}^{\dagger} j_{\nu z}$ we have

$$j_{\nu z}^{\dagger} j_{\nu z} = b^2 \left(\sin \chi \frac{\partial^2}{\partial \chi^2} \sin \chi - \cos^2 \chi + \cos \chi \frac{\partial}{\partial \chi} \sin \chi \right.$$

$$- \sin \chi \frac{\partial}{\partial \chi} \cos \chi \bigg). \tag{13}$$

The local functions $\sin \chi$ and $\cos \chi$ are diagonal,

$$\langle \xi_{n'}(\chi) | \cos \chi | \xi_n(\chi) \rangle$$

$$= \delta_{n'n} \cos(n\Delta) \quad \text{and} \quad \langle \xi_{n'}(\chi) | \sin \chi | \xi_n(\chi) \rangle$$

$$= \delta_{n'n} \sin(n\Delta). \tag{14}$$

The derivatives are given by[76,77]

$$\left\langle \xi_{n'} \left| \frac{\partial}{\partial \chi} \right| \xi_n \right\rangle = \begin{cases} 0 & \text{for } n' = n \\ \dfrac{(-1)^{n'-n}}{(n'-n)\Delta} & \text{for } n' \neq n. \end{cases} \tag{15}$$

As in the theory of the asymmetric rotor we will find it convenient in the computation of matrix elements to write H^{rot} in terms of J_z and $J_{\pm} \equiv J_x \mp J_y$ (this definition is due to the anomalous commutation relations satisfied by the J_i), thus

$$H^{\text{rot}} = \tfrac{1}{2}(A+B)J^2 + [C - \tfrac{1}{2}(A+B)]J_z^2$$

$$+ \tfrac{1}{4}(A-B)(J_+^2 + J_-^2). \tag{16}$$

The numerical values: $(A+B)/2 = 0.173$ cm^{-1}, $C - (A+B)/2 = -0.098$ cm^{-1}, and $(A-B)/4 = 0.032$ cm^{-1}. We write here H^{rot} as the Hamiltonian of a rigid rotor close to an oblate top for which $A = B$, as we did for the water trimer, i.e., $K \equiv K_c$. Although in this case B is closer to C than to A, we find it convenient to have the z-axis perpendicular to the plane of the trimer rather than along the x-axis (a-axis) of Fig. 1, what we would have to do if we wrote the Hamiltonian in a form close to the prolate limit. Note that, since $C - (A+B)/2$ is negative and $(A-B)/4$ is fairly small, the eigenvalues of H^{rot} may be expected to increase with decreasing eigenvalues of J_z^2.

After the Hamilton matrix is computed in the manner just described, we determine its lowest eigenvectors and eigenvalues by means of the routine DSPEVX in the LAPACK library.[78]

TABLE IV. The lowest ten $J=0$ excitation energies. All energy units are cm^{-1}. The first column gives the symmetry of the state under E^*. Column two is for the protonated trimer and is computed from a potential including the pair potential only, cf. Eq. (6). The third column includes the nonadditive three-body effects. The last column is for the deuterated trimer and is obtained from the pair plus three-body potential. Absolute values of zero point energies D_0 for the protonated species are 3449.68 (pair) and 3968.78 (total). The corresponding D_e values are 3629.17 and 4164.26. For the deuterated species, $D_0 = 4014.04$.

| Sym.	H₂O(pair)	H₂O(total)	D₂O(total)
A_1	0.00	0.00	0.00
A_2	14.40	8.94	1.39
A_2	125.91	129.19	95.07
A_1	136.41	135.78	95.73
A_1	181.00	196.58	162.92
A_2	258.95	270.72	192.36
A_1	270.87	277.35	197.66
A_2	282.17	283.99	198.81
A_2	324.95	334.75	255.06
A_1	382.03	392.28	271.76

V. RESULTS AND DISCUSSION

No symmetry was used in the calculations other than in choosing the *ab initio* points on the PES and the fit of this surface. In order to understand the results it is necessary to say first a few words on the symmetry of the problem.

A. Symmetry considerations

In our model, where we have different *fixed* angles ξ_1 and ξ_2 and fixed monomer positions, the two water molecules are distinguishable. Furthermore the model does not allow for the intramolecular permutations of the protons. In other words, the identity E and inversion E^* are the only symmetry operations left of all the elements in the complete permutation-inversion group. Inversion with respect to the center of mass of the trimer sends the Euler angle γ to $\gamma + \pi$, and gives $\chi_1 \mapsto -\chi_1$ and $\chi_2 \mapsto -\chi_2$. When we neglect H^{Cor} the exact eigenfunctions are products of eigenfunctions of H^{rot} (asymmetric top functions) and of H^{int}. The symmetry of the total eigenfunctions is an outer product of the symmetries of the eigenfunctions of both operators. When we do include Coriolis interaction, in principle only the symmetry of the total wave function is determined. We will find, however, that this interaction is small and that the symmetries imposed by H^{int} and H^{rot} separately are still clearly recognizable in the wave functions.

B. $J=0$ states

The lowest 10 energies for the $J=0$ states are given in Table IV. We tested grid spacings and grid sizes and found that the lowest four states have converged to within 0.01 cm^{-1}, while from the fifth state onward the errors are slowly increasing, with a largest error of 0.4 cm^{-1} for the tenth state. Hence we conclude that a grid spacing of 10° and a grid with χ_1 and χ_2 ranging from $-110°$ to $110°$ is sufficiently accurate for our purpose. The zero point vibrational energy $D_e - D_0$ is 195.53 cm^{-1}. Note also the importance of three-body effects in the potential on the tunnel splitting. In Table IV we see that neglect of these effects in the PES
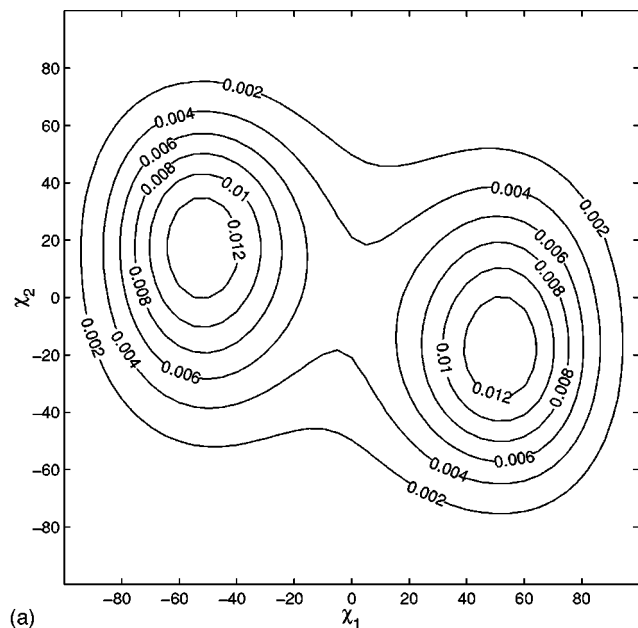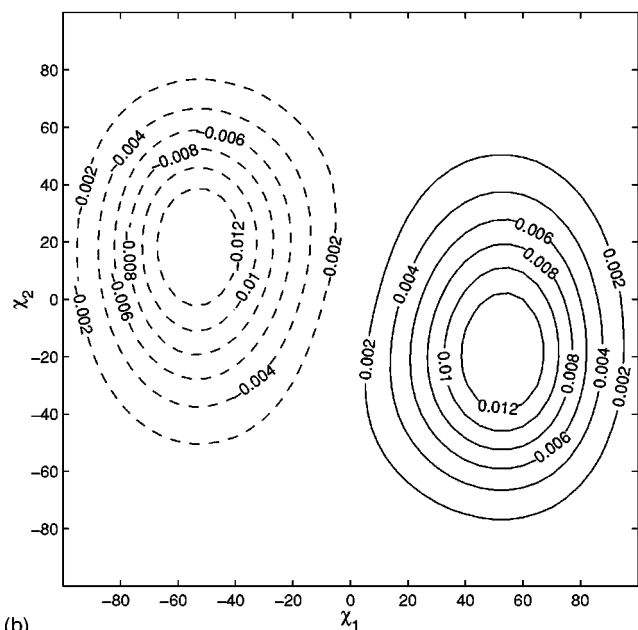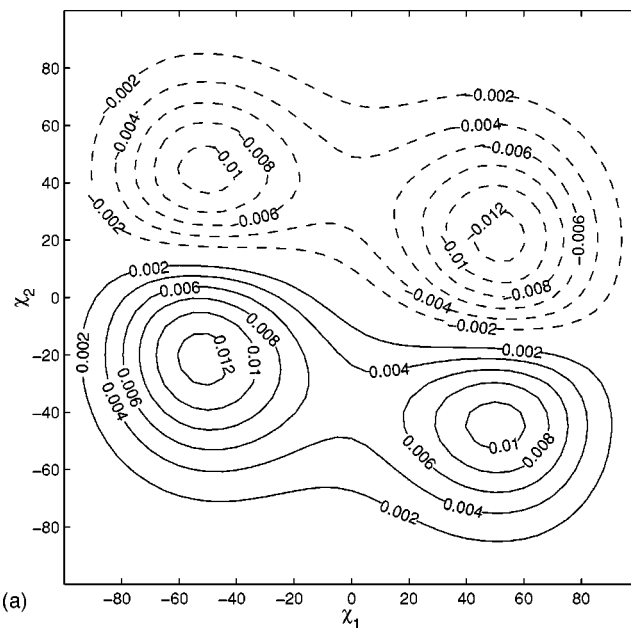
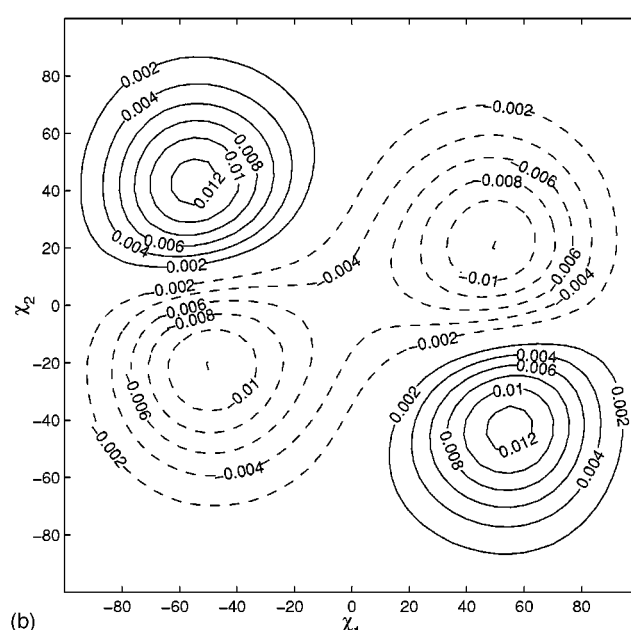FIG. 3. Contour diagrams of the ground state wave function and the first excited tunneling state as a function of the angles χ_1 and χ_2. The second state has an energy 8.94 cm^{-1} above the first.

FIG. 4. Contour diagram of the first excited vibrational wave function and its tunnel splitted counterpart as a function of the angles χ_1 and χ_2. The energies are 135.78 and 129.19 cm^{-1}, respectively. The tunnel splitting is 6.59 cm^{-1}.

increases the splitting from 8.94 to 14.40 cm^{-1}, which is consistent with the fact, noted above, that the barrier height in the two-body potential is 62 cm^{-1} lower than in the total potential. See Fig. 3 for the A_1 ground state and the first A_2 tunneling state, which is 8.94 cm^{-1} higher than the ground state.

The first excited A_1 vibrational state is shown at the top of Fig. 4. We determined a one-dimensional force constant by fitting a parabola through the PES as a function of χ_2 at fixed $\chi_1 = 57°$. The harmonic energy obtained by this force constant is 136.75 cm^{-1}. This value agrees well with the energy 135.78 cm^{-1} of the state at the top of Fig. 4. We conclude that this state resembles the first excited state of a harmonic oscillator moving in the χ_2 direction. The tunnel splitted A_2 counterpart is also shown in Fig. 4. Its energy is 6.59 cm^{-1} lower. The overtones of this motion are shown in Fig. 5. Here the antisymmetric state is 6.78 cm^{-1} above the symmetric one.

We see here that the system separates reasonably well in a χ_1 and a χ_2 dependent part. The motion in the χ_2 direction has a zero point energy of approximately $135.78/2 \approx 68$ cm^{-1}. The zero point energy for the perpendicular motion in the χ_1 direction is then $195.53 - 68 \approx 128$ cm^{-1}, so that states with energies larger than ~ 185 cm^{-1} are above the barrier. The motion that crosses the barrier is predominantly in the χ_1 direction.

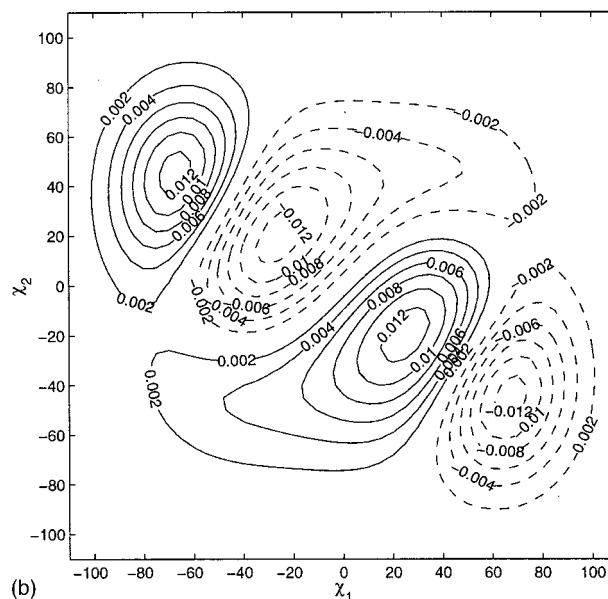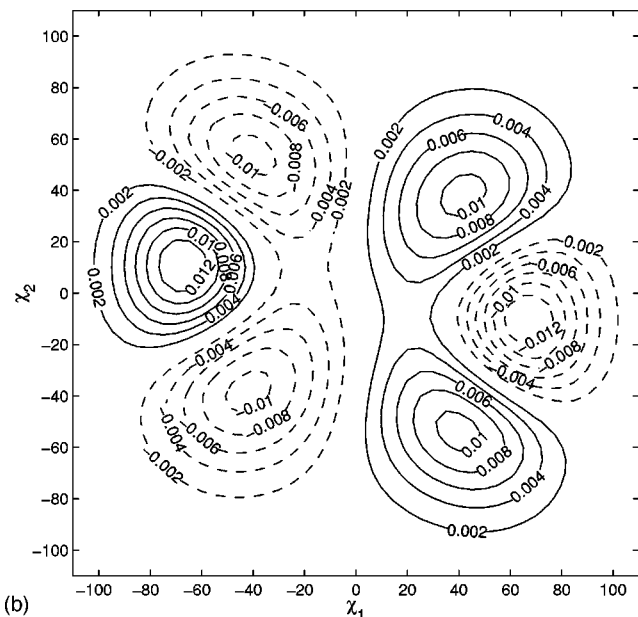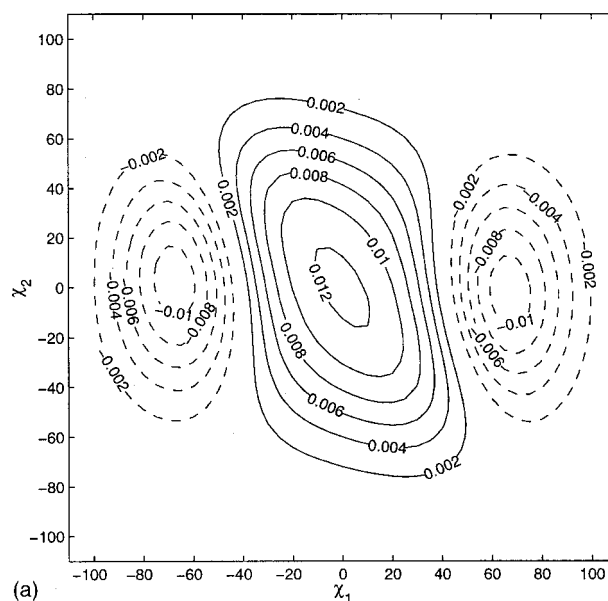In the top part of Fig. 6 we show a wave function of

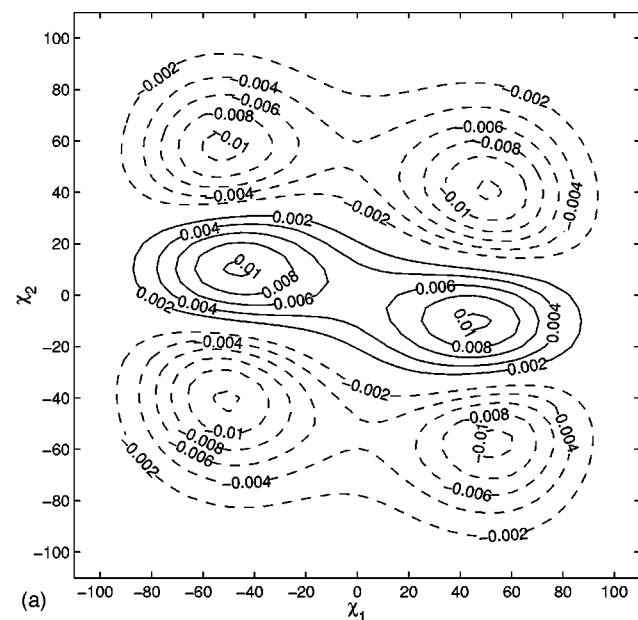FIG. 5. Contour diagram of first overtone vibrational wave function and its tunnel splitted counterpart as a function of the angles χ_1 and χ_2. The energies are 277.35 and 283.99 cm^{-1}, respectively. The tunnel splitting is 6.64 cm^{-1}.

FIG. 6. Contour diagrams of the symmetric wave function at 196.58 cm^{-1} and its antisymmetric tunnel counterpart at 270.72 cm^{-1} as a function of the angles χ_1 and χ_2. The tunnel splitting is 74.14 cm^{-1}.

energy 196.58 cm^{-1} that has two distinct nodal planes parallel to the χ_2 axis, i.e., it oscillates in the χ_1 direction. It is heavily modified by tunneling, as also follows from the large tunnel splitting of 74.18 cm^{-1}. Finally we note that the assignment of the antisymmetric functions shown in Figs. 6 and 5 is not unambiguous. The two states mix heavily, since they are in the same energy regime.

C. $J \neq 0$ states

We give a brief discussion of the $J \neq 0$ states and investigate in particular the contribution of the Coriolis interaction H^{Cor}, cf. Eq. (4). This contribution is given by

$$E_{ki}^{\text{Cor}} = E_{ki}^{\text{total}} - E_k^{\text{rot}} - E_i^{\text{int}}, \tag{17}$$

where the first term on the right hand side is an eigenvalue of the total $(2J+1)N_{\text{grid}}$-dimensional H-matrix. The second term is obtained by diagonalizing the matrix of H^{rot} in a basis of eigenfunctions of J^2 and J_z, $K = -J, \ldots, J$. The last term is an eigenvalue of H^{int} obtained for $J=0$ in a basis of N_{grid} sinc functions. We considered a $10°$ grid spacing on the interval $[-110°, 110°]$, thus we have $N_{\text{grid}} = 23^2 = 529$ sinc functions. We computed only the lowest ten vibrational-tunneling states. For $J=1$ and $J=2$ the Coriolis interaction E_{ki}^{Cor} is very nearly the same for each of the vibrational-tunneling states (at least for $i \leqslant 10$) and depends only on k. For $J=1$ the values are -0.0032, -0.0022, -0.0053 cm^{-1}, while for $J=2$ they are -0.0015, -0.0054, -0.0150, -0.0141, and -0.0176 cm^{-1}. In both cases the

Coriolis interactions are listed for increasing rigid rotor energy. Clearly, for low J quantum numbers this interaction is small. However, in high-resolution spectroscopy even the small Coriolis effects may be discerned. If these will be observed in the future we will—guided by the experiments—return to our calculations and compute the Coriolis interactions with more accuracy. We can then also consider the vibrational dependence of the rotational constants by computing them as expectation values of the inverse inertia tensor over different vibrational states.

D. The deuterated trimer

In order to obtain some insight in the effect of the atomic masses and especially the masses of the rotating hydrogens on the tunnel splitting, we replaced all protons (including the one on HCl) by deuterons [mass 2.013 553 212 71 u, Ref. 79]. This substitution changes the center of mass of the trimer as well as of the monomers and accordingly a number of the parameters other than the masses in the kinetic energy expression will be changed, too. However, these changes will be small compared to the doubling of the mass of the flipping protons and hence we neglected them. We get new values for I_{xx} and I_{xy}, where the former tensor element is the most important quantity determining the spectrum; its numerical value for the deuterated species is given by $1/(2I_{xx})$ $= 11.581$ cm^{-1}. Using this value we find as the first tunnel splitting 1.39 cm^{-1} (was 8.94 cm^{-1}), while the second tunnel splitting is 0.67 cm^{-1}, which was 6.59 cm^{-1}. The lowest energy is at -4014.04 cm^{-1}, so that the zero point energy $D_e - D_0$ is 150.22 cm^{-1}, about 45 cm^{-1} lower than for the protonated isotopomer. The first vibrational excitation is at 95.07 cm^{-1}, which may be compared with the corresponding value of 129.19 cm^{-1} for the protonated species. Evidently, the doubling of the hydrogen masses has a drastic effect on the VRT levels just as for the water trimer.[54]

VI. CONCLUDING REMARKS

We have made a first exploration of the VRT levels of the system HCl–$(H_2O)_2$. We took an experimental geometry and computed an *ab initio* potential energy surface as a function of two rotational angles. These angles describe the flipping of the nonhydrogen-bonded hydrogens through the plane of the trimer. Our results will be a useful guide for future measurements of the VRT spectrum. We predict a tunnel splitting of 8.94 cm^{-1}. The transition from the A_1 ground state to the A_2 tunnel splitted level is dipole allowed and should be observable in the far-infrared. The deuterated species has a corresponding tunnel splitting of 1.39 cm^{-1}, which also should be observable. We computed vibrational levels which are also tunnel splitted. The states excited in the χ_2 direction show splittings of about 6.6 cm^{-1}, while the first excited vibrational state in the χ_1 direction has the much larger splitting of about 74 cm^{-1}.

We considered Coriolis interactions between the internal motions and the overall rotation of the trimer. We found this interaction to be very small. So, a good approximation of the VRT levels for low J can be obtained from a separate diagonalization of the asymmetric rigid rotor Hamiltonian and the internal Hamiltonian for $J=0$.

Finally, we found that three-body effects in the potential are very important. Neglect of these effects changes the first tunnel splitting from 8.94 to 14.40 cm^{-1}.

[1] T. R. Dyke and J. S. Muenter, J. Chem. Phys. **60**, 2929 (1974).
[2] E. Zwart, J. J. ter Meulen, W. L. Meerts, and L. H. Coudert, J. Mol. Spectrosc. **147**, 27 (1991).
[3] G. T. Fraser, Int. Rev. Phys. Chem. **10**, 189 (1991).
[4] N. Pugliano and R. J. Saykally, J. Chem. Phys. **96**, 1832 (1992).
[5] N. Pugliano, J. D. Cruzan, J. G. Loeser, and R. J. Saykally, J. Chem. Phys. **98**, 6600 (1993).
[6] J. B. Paul, R. A. Provencal, and R. J. Saykally, J. Phys. Chem. A **102**, 3279 (1998).
[7] L. B. Braly, J. D. Cruzan, K. Liu, R. S. Fellers, and R. J. Saykally, J. Chem. Phys. **112**, 10293 (2000).
[8] L. B. Braly, K. Liu, M. G. Brown, F. N. Keutsch, and R. J. Saykally, J. Chem. Phys. **112**, 10314 (2000).
[9] K. Liu *et al.*, J. Am. Chem. Soc. **116**, 3507 (1994).
[10] M. R. Viant *et al.*, J. Phys. Chem. A **101**, 9032 (1997).
[11] M. R. Viant, M. G. Brown, J. D. Cruzan, and R. J. Saykally, J. Chem. Phys. **110**, 4369 (1999).
[12] M. G. Brown, M. R. Viant, R. P. McLaughlin, C. J. Keoshian, E. Michael, J. D. Cruzan, and R. J. Saykally, J. Chem. Phys. **111**, 7789 (1999).
[13] J. D. Cruzan, M. R. Viant, M. G. Brown, and R. J. Saykally, J. Phys. Chem. A **101**, 9022 (1997).
[14] K. Liu, M. G. Brown, J. D. Cruzan, and R. J. Saykally, J. Phys. Chem. A **101**, 9011 (1997).
[15] M. G. Brown, F. N. Keutsch, and R. J. Saykally, J. Chem. Phys. **109**, 9645 (1998).
[16] K. Liu, M. G. Brown, and R. J. Saykally, J. Phys. Chem. A **101**, 8995 (1997).
[17] A. van der Avoird, P. E. S. Wormer, and R. Moszynski, Chem. Rev. **94**, 1931 (1994).
[18] P. E. S. Wormer and A. van der Avoird, Chem. Rev. **100**, 4109 (2000).
[19] R. S. Fellers, L. B. Braly, R. J. Saykally, and C. Leforestier, J. Chem. Phys. **110**, 6306 (1999).
[20] H. Chen, S. Liu, and J. C. Light, J. Chem. Phys. **110**, 168 (1999).
[21] G. C. Groenenboom, E. M. Mas, R. Bukowski, K. Szalewicz, P. E. S. Wormer, and A. van der Avoird, Phys. Rev. Lett. **84**, 4072 (2000).
[22] G. C. Groenenboom, P. E. S. Wormer, A. van der Avoird, E. M. Mas, R. Bukowski, and K. Szalewicz, J. Chem. Phys. **113**, 6702 (2000).
[23] M. J. Molina, T.-L. Tso, L. T. Molina, and F. C.-Y. Wang, Science **238**, 1253 (1987).
[24] D. C. Clary, Science **271**, 1509 (1996).
[25] F. M. Geiger, J. M. Hicks, and A. C. de Dios, J. Phys. Chem. A **102**, 1514 (1998).
[26] G. J. Kroes and D. C. Clary, J. Phys. Chem. **96**, 7079 (1992).
[27] G. J. Kroes and D. C. Clary, Geophys. Res. Lett. **19**, 1355 (1992).
[28] G. Bussolin, S. Casassa, C. Pisani, and P. Ugliengo, J. Chem. Phys. **108**, 9516 (1998).
[29] A. Al-Halabi, A. W. Kleyn, and G. J. Kroes, Chem. Phys. Lett. **307**, 505 (1999).
[30] S. Elliot, R. P. Turco, O. B. Toon, and P. Hamill, J. Atmos. Chem. **13**, 211 (1991).
[31] L. Delzeit, B. Rowland, and J. P. Devlin, J. Phys. Chem. **97**, 10312 (2000).
[32] J. D. Graham and J. T. Roberts, J. Phys. Chem. **98**, 5974 (1994).
[33] N. Materer *et al.*, J. Phys. Chem. **99**, 6267 (1995).
[34] M. J. Isakson and G. O. Sitz, J. Phys. Chem. A **103**, 2044 (1999).
[35] J. G. C. M. van Duijneveldt-van de Rijdt and F. B. van Duijneveldt, Chem. Phys. **175**, 271 (1993).
[36] W. Klopper and M. Schütz, Chem. Phys. Lett. **237**, 536 (1993).
[37] D. J. Wales, J. Am. Chem. Soc. **115**, 11180 (1993).
[38] D. J. Wales, J. Am. Chem. Soc. **115**, 11119 (1993).

[39] S. S. Xantheas and T. H. Dunning, Jr., J. Chem. Phys. **99**, 8774 (1993).

[40] S. S. Xantheas and T. H. Dunning, Jr., J. Chem. Phys. **98**, 8037 (1993).

[41] M. Schütz, T. Bürgi, S. Leutwyler, and H. B. Bürgi, J. Chem. Phys. **99**, 5228 (1993).

[42] M. Schütz, T. Bürgi, S. Leutwyler, and H. B. Bürgi, J. Chem. Phys. **100**, 1780 (1994).

[43] S. S. Xantheas, J. Chem. Phys. **100**, 7523 (1994).

[44] J. K. Gregory and D. C. Clary, Chem. Phys. Lett. **228**, 547 (1994).

[45] J. K. Gregory and D. C. Clary, J. Chem. Phys. **103**, 8924 (1995).

[46] J. K. Gregory and D. C. Clary, J. Chem. Phys. **102**, 7817 (1995).

[47] J. G. C. M. van Duijneveldt-van de Rijdt and F. B. van Duijneveldt, Chem. Phys. Lett. **237**, 560 (1995).

[48] T. Bürgi, S. Graf, S. Leutwyler, and W. Klopper, J. Chem. Phys. **103**, 1077 (1995).

[49] W. Klopper, M. Schütz, H.-P. Lüthi, and S. Leutwyler, J. Chem. Phys. **103**, 1085 (1995).

[50] J. E. Fowler and H. F. Schaefer, J. Am. Chem. Soc. **117**, 446 (1995).

[51] W. Klopper and M. Schütz, Chem. Phys. Lett. **237**, 536 (1995).

[52] D. Sabo, Z. Bačić, T. Bürgi, and S. Leutwyler, Chem. Phys. Lett. **244**, 283 (1995).

[53] A. van der Avoird, E. H. T. Olthof, and P. E. S. Wormer, J. Chem. Phys. **105**, 8034 (1996).

[54] E. H. T. Olthof, A. van der Avoird, P. E. S. Wormer, K. Liu, and R. J. Saykally, J. Chem. Phys. **105**, 8051 (1996).

[55] D. Sabo, Z. Bačić, S. Graf, and S. Leutwyler, Chem. Phys. Lett. **261**, 318 (1996).

[56] T. R. Walsh and D. J. Wales, J. Chem. Soc., Faraday Trans. **92**, 2505 (1996).

[57] J. M. Sorenson, J. K. Gregory, and D. C. Clary, Chem. Phys. Lett. **263**, 680 (1996).

[58] D. J. Wales and T. R. Walsh, J. Chem. Phys. **106**, 7193 (1997).

[59] M. P. Hodges, A. J. Stone, and S. S. Xantheas, J. Phys. Chem. A **101**, 9163 (1997).

[60] A. Milet, R. Moszynski, P. E. S. Wormer, and A. van der Avoird, J. Phys. Chem. A **103**, 6811 (1999).

[61] M. Geleijns and A. van der Avoird, J. Chem. Phys. **110**, 823 (1999).

[62] D. Sabo, Z. Bačić, S. Graf, and S. Leutwyler, J. Chem. Phys. **110**, 5745 (1999).

[63] D. Sabo, Z. Bačić, S. Graf, and S. Leutwyler, J. Chem. Phys. **111**, 5331 (1999).

[64] D. Sabo, Z. Bačić, S. Graf, and S. Leutwyler, J. Chem. Phys. **111**, 10727 (1999).

[65] D. J. Wales, in *Advances in Molecular Vibrations and Collision Dynamics*, edited by J. M. Bowman and Z. Bačić (JAI, Stamford, 1998), p. 365.

[66] A. Milet, C. Struniewicz, R. Moszynski, and P. E. S. Wormer, Theor. Chem. Acc. **104**, 195 (2000).

[67] Z. Kisiel, E. Białkowska-Jaworska, L. Pszczółkowski, A. Milet, C. Struniewicz, R. Moszynski, and J. Sadlej, J. Chem. Phys. **112**, 5767 (2000).

[68] B. Podolsky, Phys. Rev. **32**, 812 (1928).

[69] MOLPRO is a package of *ab initio* programs written by H.-J. Werner and P. J. Knowles, with contributions from R. D. Amos, A. Berning, D. L. Cooper *et al.*

[70] Basis sets were obtained from the Extensible Computational Chemistry Environment Basis Set Database, Version 1.0, as developed and distributed by the Molecular Science Computing Facility, Environmental and Molecular Sciences Laboratory which is part of the Pacific Northwest Laboratory, P.O. Box 999, Richland, Washington 99352, USA, and funded by the U.S. Department of Energy. The Pacific Northwest Laboratory is a multi-program laboratory operated by Battelle Memorial Institute for the U.S. Department of Energy under Contract No. DE-AC06-76RLO 1830.

[71] J. G. C. M. van Duijneveldt-van de Rijdt and F. B. van Duijneveldt, J. Chem. Phys. **97**, 5019 (1992).

[72] A. D. McLean and G. S. Chandler, J. Chem. Phys. **72**, 5639 (1980).

[73] See EPAPS Document No. E-JCPSA6-115-011132 for the raw CCSD(T) pair- and three-body energies on the grid. This document may be retrieved via the EPAPS homepage (http://www.aip.org/pubservs/epaps.html) or from ftp.aip.org in the directory/epaps/. See the EPAPS homepage for more information.

[74] T.-S. Ho and H. Rabitz, J. Chem. Phys. **104**, 2584 (1996).

[75] L. C. Biedenharn and J. D. Louck, *Angular Momentum in Quantum Physics*, Vol. 8 in *Encyclopedia of Mathematics* (Addison–Wesley, Reading, 1981).

[76] D. T. Colbert and W. H. Miller, J. Chem. Phys. **96**, 1982 (1992).

[77] G. C. Groenenboom and D. T. Colbert, J. Chem. Phys. **99**, 9681 (1993).

[78] E. Anderson, Z. Bai, C. Bischof *et al.*, *LAPACK Users' Guide*, 3rd ed. (Society for Industrial and Applied Mathematics, Philadelphia, 1999).

[79] P. J. Mohr and B. N. Taylor, Phys. Today **53**, BG6 (2000).